Protonation and Zn(II) Coordination by Dipyridine-Containing Macrocycles with Different Molecular Architecture. A Case of pH-Controlled Metal Jumping Outside−Inside the Macrocyclic Cavity

Carlos Lodeiro,[†] A. Jorge Parola,[†] Fernando Pina,*[,†] Carla Bazzicalupi,[‡] Andrea Bencini,*[,‡] Antonio Bianchi,*[,‡] Claudia Giorgi,[‡] Andrea Masotti,[‡] and Barbara Valtancoli[‡]

Departamento de Química, Centro de Química Fina e Biotecnologia, Faculdade de Ciências e Tecnologia, Universidade Nova de Lisboa, Quinta da Torre 2825 Monte de Caparica, Portugal, and Department of Chemistry, University of Florence, Via Maragliano 75/77, 50144 Florence, Italy

Received December 7, 2000

The synthesis of the macrocyclic ligand 4,4′-(2,5,8,11,14-pentaaza[15])-2,2′-bipyridylophane (**L3**), which contains a pentaamine chain linking the 4,4′-positions of a 2,2′-dipyridine moiety, is reported. Protonation and Zn(II) complexation by **L3** and by macrocycle **L2**, containing the same pentaamine chain connecting the 6,6′-positions of 2,2′-dipyridine, were studied by means of potentiometric, UV−vis, and fluorescent emission measurements. While in **L2** all the nitrogen donor atoms are convergent inside the macrocyclic cavity, in **L3** the heteroaromatic nitrogen atoms are located outside. Both ligands form mono- and dinuclear Zn(II) complexes in aqueous solution. In the mononuclear Zn(II) complexes with **L2**, the metal is coordinated inside the macrocyclic cavity, bound to the heteroaromatic nitrogen donors and three amine groups of the aliphatic chain. As shown by the crystal structure of the $[Zn\mathbf{L2}]^{2+}$ complex, the two benzylic nitrogens are not coordinated and facile protonation of the complex takes place at slightly acidic pH values. Considering the mononuclear $[Zn\mathbf{L3}]^{2+}$ complex, the metal is encapsulated inside the cavity, not coordinated by the dipyridine unit. Protonation of the complex occurs on the aliphatic polyamine chain and gives rise to translocation of the metal outside the cavity, bound to the heteroaromatic nitrogens.

Introduction

Macrocyclic ligands containing various binding functionalities are the subject of current interest due to their ability to selectively bind, transform, and transfer a large variety of substrates from charged species[1−22] to neutral molecules.[23] Structural factors, such as ligand rigidity, type of donor atoms, and their disposition, have been shown to play significant roles in determining the binding features of macrocycles toward metal cations.[1−13] Heteroaromatic subunits, such as 2,2′-dipyridine or 1,10-phenanthroline, are often introduced as integral parts of the host molecules.[24,25] Incorporation of these moieties into macrocyclic structures allows one to combine within the same

* Corresponding authors. E-mail for F. Pina: fjp@dq.fct.unl.pt. E-mail for A. Bencini: benc@chim1.unifi.it.
[†] Universidade Nova de Lisboa.
[‡] University of Florence.

(1) (a) Bradshaw, J. S. *Aza-crown Macrocycles*, Wiley: New York, 1993. (b) Krakowiak K. E.; Bradshaw J. S.; Zamecka-Krakowiak, D. J. *Chem. Rev.* **1989**, *89*, 929. (c) Izatt, R. M.; Pawlak, K.; Bradshaw J. S. *Chem. Rev.* **1995**, *95*, 5**,** 2529.
(2) Gokel, G. W. *Crown Ethers and Cryptands;* Stoddart, J. F., Ed.; The Royal Society of Chemistry: Cambridge, UK, 1991.
(3) Lehn, J. M. *Supramolecular Chemistry;* VCH: New York, 1995.
(4) Guerriero, P.; Tamburini, S.; Vigato, P. A. *Coord. Chem. Rev.* **1995**, *110*, 17.
(5) Nation, D. A.; Martell, A. E.; Carroll, R. I.; Clearfield A. *Inorg. Chem.* **1996**, *35*, 7246 and references therein.
(6) Lindoy, L. F. *The Chemistry of Macrocyclic Ligand Complexes;* Cambridge University Press: Cambridge, UK, 1989.
(7) Lindoy, L. F. *Pure Appl. Chem.* **1997**, *69*, 2179.
(8) (a) Amendola, V.; Fabbrizzi, L.; Mangano, C.; Pallavicini, P.; Perotti, A.; Taglietti, A. *J. Chem. Soc, Dalton Trans.* **2000**, 185 and references therein. (b) Fabrizzi L. (Ed.) Luminescent Sensors. *Coord. Chem. Rev.*, **2000**, Vol. 205.
(9) Kaden, T. A.; Tschudin, D.; Studer M.; Brunner, U. *Pure Appl. Chem.*, **1989**, *61*, 879.
(10) Kaden, T. A. *Pure Appl. Chem.* **1988**, *60*, 117.
(11) Blake, A. J.; Champness, N. R.; Hubberstey, P.; Li, W. S.; Schröder, M.; Withersby, M. A. *Coord. Chem. Rev.*, **1999**, *183*, 117.
(12) Nelson,. J.; McKee, V.; Morgan, G. In *Progress Inorganic Chemistry;* Karlin, K. D., Ed.; Wiley: New York, 1998; Vol. 47, p 167.
(13) Bazzicalupi, C.; Bencini, A.; Fusi, V.; Giorgi C.; Paoletti P.; Valtancoli, B. *Inorg. Chem.* **1998**, *37*, 941. (c) Bazzicalupi, C.; Bencini, A.; Berni, E.; Fedi, V.; Fusi, V.; Giorgi C.; Paoletti P.; Valtancoli, B. *Inorg. Chem.* **1999**, 4115.
(14) Izatt, R. M.; Pawlak, K.; Bradshaw, J. S.;. Bruenig, R. L. *Chem. Rev.* **1991**, *91*, 1721
(15) Bianchi, A.; Garcia-España, E.; Bowman-James, K. (Eds.) *Supramolecular Chemistry of Anions;* Wiley-VCH: New York, 1997.
(16) Hosseini, M. W.; Blaker, A. J.; Lehn, J.-M. *J. Am. Chem. Soc.* **1990**, *112*, 3896.
(17) Aguilar, J. A.; Garcia-España, E.; Guerrero, J. A.; Luis, S. V.; Llinares, J. M.; Miravet, M. F.; Ramirez J. A.; Soriano C. *J. Chem. Soc., Chem. Commun.*, 1995, 2237.
(18) Eliseev A. V. and Schneider, H.-J. *J. Am. Chem. Soc.* **1994**, *116*, 6081 and references therein.
(19) (a) Bazzicalupi, C.; Beconcini, A.; Bencini, A, Fusi, V.; Giorgi, C.; Masotti, A.; Valtancoli, B. *J. Chem. Soc., Perkin Trans. 2* **1999**, 1675. (b) Bazzicalupi, C.; Bencini, A.; Bianchi, A.; Cecchi, M.; Escuder, B.; Fusi, V.; E. Garcia-España, Giorgi, C.; S. V. Luis, Maccagni, G.; Marcelino, V.; Paoletti, P.; Valtancoli, B. *J. Am. Chem. Soc.* **1999**, *121*, 6807.
(20) (a) Mertes, M. P.; Mertes, K. B. *Acc. Chem. Res.* **1990**, *23*, 413. (b) Mason, S.; Clifford, T.; Seib, L.; Kuzcera, K.; Bowman-James, K. *J. Am. Chem. Soc.* **1998**, *120*, 8899.
(21) Kràl, V.; Furuta, H.; Shreder, K.; Lynch, V.; Sessler, J. L. *J. Am. Chem. Soc.* **1996**, *118*, 1595.
(22) Balzani, V.; Credi, A.; Raymo, F. M.; Stoddart, J. F. *Angew. Chem., Int. Ed.* **2000**, *39*, 3348 and references therein
(23) Izatt, R. M.; Bradshaw J. S.; Pawlak, K.; Bruening, R. L.; Tarbet, *Chem. Rev.* **1992**, *92*, 2**,** 1261.

10.1021/ic001381k CCC: $20.00
Published on Web 05/15/2001

Scheme 1

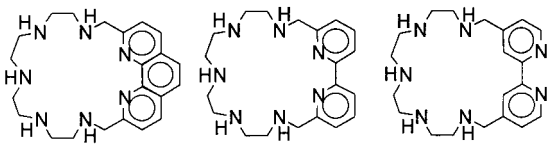

L1 **L2** **L3**

ligand the special complexation features of macrocycles with the photophysical and photochemical properties displayed by the metal complexes of these heterocycles.[26,27]

Recently, we reported on the synthesis and metal-coordination characteristics of a new series of polyamine macrocycles, such as **L1** (Scheme 1),[28a] containing a polyamine chain linking the 2,9-positions of phenanthroline.[28,29]

A previous investigation on the Zn(II) coordination properties of these ligands revealed that insertion of a rigid phenanthroline unit within a macrocyclic framework precludes the simultaneous participation of the heteroaromatic donors and the benzylic amine groups in metal binding.[29] As a matter of fact, in the Zn(II) complexes, the metal is coordinated to the phenanthroline nitrogens and not bound, or weakly bound, to the benzylic nitrogens. Consequently, the expected fluorescence emission of the Zn(II) complexes is quenched by an electron-transfer process involving the unprotonated benzylic amines.

We have now extended this study to polyamine macrocycles incorporating a dipyridine unit, such **L2** and **L3**. Both of them contain two different binding moieties, a pentaamine chain and a dipyridine moiety. While in **L2** the disposition of the heteroaromatic and aliphatic nitrogen donors is convergent toward the macrocyclic cavity, in **L3** the two aromatic nitrogens point outside the cavity. This molecular architecture defines two well-separated binding zones, the macrocyclic cavity and the external dipyridine unit. Since the process of metal coordination is competitive with ligand protonation and aliphatic nitrogens are usually more basic than heteroaromatic ones,[30] we hoped that the metal could change its coordination site, translating from inside to outside the macrocyclic cavity upon protonation of the aliphatic amine groups.

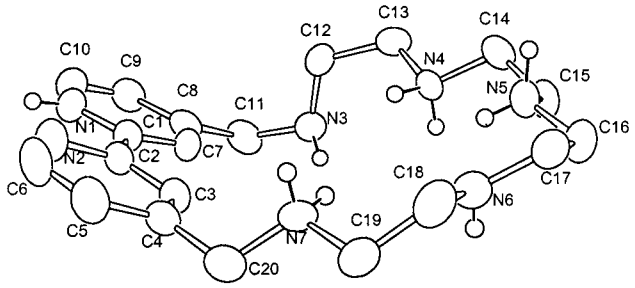

Figure 1. ORTEP drawing of the $[H_4\mathbf{L3}]^{4+}$ cation.

Table 1. Protonation Constants (log *K*) of Ligands L2 and L3 (0.1 M NMe_4Cl, 298.1 K)

reaction	log *K* **L2**	**L3**
$\mathbf{L} + H^+ = [H\mathbf{L}]^+$	9.42(1)	9.62(5)
$[HL]^+ + H^+ = [H_2\mathbf{L}]^{2+}$	8.76(1)	8.34(5)
$[H_2L]^{2+} + H^+ = [H_3\mathbf{L}]^{3+}$	7.37(2)	6.40(8)
$[H_3L]^{3+} + H^+ = [H_4\mathbf{L}]^{4+}$	4.16(2)	4.57(9)
$[H_4L]^{4+} + H^+ = [H_5\mathbf{L}]^{5+}$	2.23(3)	3.2(1)
$[H_5L]^{5+} + H^+ = [H_6\mathbf{L}]^{6+}$	1.5(1)	2.9(1)
$[H_6L]^{6+} + H^+ = [H_7\mathbf{L}]^{7+}$		2.5(1)

Results and Discussion

Ligand Protonation. Crystal Structure of $[H_4\mathbf{L3}](ClO_4)_4\cdot H_2O$. The molecular structure of $[H_4\mathbf{L3}](ClO_4)_4\cdot H_2O$ consists of protonated cations $[H_4\mathbf{L3}]^{4+}$, perchlorate anions, and water solvent molecules. An ORTEP[31] drawing of the $[H_4\mathbf{L3}]^{4+}$ cation is shown in Figure 1. The ΔF map allows determination of the positions of the N−H protons. In this tetraprotonated cation, three acidic protons are localized on the N4, N5, and N7 aliphatic nitrogen donors and one on the dipyridine nitrogen atom N1.

Considering the ligand conformation, the aliphatic chain assumes a rather flat conformation, the five nitrogens N3−N7 being almost coplanar. Such a disposition is probably due to the electrostatic repulsions between the positive charges of protonated nitrogens. The two aromatic rings of dipyridine are also almost coplanar (dihedral angle 2.4(2)°). The mean plane defined by the five amine groups N3−N7 (max deviation of 0.385(6) Å for N6) forms an angle of 42.4(1)° with the plane of the heteroaromatic unit, giving rise to an overall bent conformation of the protonated ligand.

Solution Studies. The protonation equilibria of **L2** and **L3** have been studied by means of potentiometric measurements in aqueous solution (0.1 mol dm^{-3} NMe_4Cl, 298.1 K), and the results are reported in Table 1. Although **L2** and **L3** contain the same types of protonable nitrogen atoms, the two ligands display a different protonation behavior. **L2** can bind up to five protons in the pH range investigated by potentiometry (2.5−10.5). A sixth protonation step was monitored below pH 2 (log

(24) Examples of previous reports on bipirydine- or phenanthroline-containing macrocycles or macrobicycles: (a) Rodriguez-Ubis, J.-C.; Alpha, B.; Plancherel, D.; Lehn, J. M. *Helv. Chim. Acta* **1984**, *67*, 2264. (b) Alpha, B.; Lehn, J. M.; Mathis, G. *Angew. Chem., Int. Ed. Engl.* **1987**, *26*, 266. (c) Cesario, M.; Guilhem, J.; Pascard, E.; Anklam, E.; Lehn, J. M.; Pietraskiewicz, M., *Helv. Chim. Acta* **1991**, *74*, 1157. (d) Bkouche-Waksmann, J.; Guilhem, J.; Pascard, E.; Alpha, B.; Deshenaux, Lehn, J. M., *Helv. Chim. Acta* **1991**, *75*, 1163. (e) Lehn, J. M.; Regnouf de Vains, J. B. *Helv. Chim. Acta* **1992**, *75*, 1221. (f) Roth, C.; Lehn, J.-M.; Guilheim, J.; Pascard, C. *Helv. Chim. Acta* **1995**, *78*, 1895 and references therein. (g) Azéma, J.; Galaup, C.; Picard, C.; Tisnès, P.; Ramos, O.; Juanes, O.; Rodrìgez-Ubis, J. C.; Brunet, E. *Tetrahedron* **2000**, *56*, 2673 and references therein. (h) Newkome, G. R.; Pappalardo, S.; Gupta, V. K:, Fronczek, F. *J. Org. Chem.* **1983**, *48*, 4848 and references therein.

(25) Vidal, P.-L.; Divisia-Blohorn, B.; Bidan, G.; Kern, J.-M.; Sauvage J.-P.; Hazemann, J.-L. *Inorg Chem.* **1999**, *38*, 4203. (b) Weck, M.; Mohr, B.; Sauvage, J.-P.; Grubbs, R. H. *J. Org. Chem.* **1999**, *64*, 5463; Rapenne, G.; Dietrich-Buchecker, C.; Sauvage, J.-P. *J. Am. Chem. Soc.* **1999**, *121*, 994. Meyer, M.;, Albrecht-Gary, A.-M.; Dietrich-Buchecker, C. O.; Sauvage, J.-P. *Inorg. Chem.* **1999**, *38*, 2279.

(26) Sammes, P. G.; Yahioglu, G. *Chem. Soc. Rev.* **1994**, 328.

(27) Barigelletti, F.; De Cola, L.; Balzani, V.; Belzer, P.; von Zelewsky, A.; Vögtle, F.; Ebmeyer, F.; Grammenudi, S. *J. Am. Chem. Soc.* **1989**, *111*, 4662; Balzani, V.; Ballardini, R.; Bolletta, F.; Gandolfi, M. T., Juris, A.; Maestri, M.; Manfrin, M. F.; Moggi, L.; Sabbatini, N. *Coord. Chem. Rev.* **1993**, *125*, 75 and references therein. (c) Sabbatini, N.; Guardigli, M.; Lehn J.-M. *Coord. Chem. Rev.* **1993**, *123*, 201. (d) Balzani, V.; Credi, A.; Venturi, M. *Coord. Chem. Rev.* **1998**, *171*, 3 and references therein.

(28) Bazzicalupi, C.; Bencini, A.; Fusi, V.; Giorgi, C.; Paoletti, P.; Valtancoli, B. *Inorg. Chem.* **1998**, *37*, 941. Bazzicalupi, C.; Bencini, A.; Fusi, V.; Giorgi, C.; Paoletti, P.; Valtancoli, B. *J. Chem. Soc., Dalton Trans.* **1999**, 393. Chand, D. K.; Schneider H.-J.; Bencini, A., Bianchi, A., Giorgi, C., Ciattini, S., Valtancoli, B. *Chem. Eur. J.* **2000**, *6*, 4001.

(29) Bazzicalupi, C.; Bencini, A.; Bianchi, A.; Fusi, V.; Giorgi, C.; Paoletti, P.; Valtancoli, B.; Pina, F.; Bernardo, M. A. *Inorg. Chem.* **1999**, *37*, 3806. Bazzicalupi, C.; Bencini, A.; Bianchi, A.; Fusi, V.; Giorgi, C.; Paoletti, P.; Valtancoli, B.; Pina, F.; Bernardo, M. A. *Eur. J. Inorg. Chem.* **1999**, 1911.

(30) Bencini, A.; Bianchi, A.; Garcia-España, E.; Micheloni M.; Ramirez, J. A. *Coord. Chem. Rev.* **1999**, *118*, 97.

(31) Johnson, C. K. ORTEP. Report ORNL-3794; Oak Ridge National Laboratory: Oak Ridge, TN, 1971.

K ca. 1.5) by means of spectrophotometric measurements. This ligand shows a marked grouping of the protonation constants, the difference between the third and the fourth protonation constant being ca. 3.2 log units. This behavior is common in macrocyclic polyamines, and it has been explained in terms of minimization of the electrostatic repulsions between the charged ammonium function.[30] On the contrary, **L3** can bind up to seven protons in aqueous solution and does not show any grouping of the protonation constants. Such a different behavior can be rationalized by considering that in **L3** protonation of dipyridine nitrogens implies the localization of positive charge outside the macrocyclic cavity, giving rise to a better minimization of the electrostatic repulsion between protonated nitrogens. Dipyridine nitrogens, however, are characterized by far lower basicity than amine nitrogens, and therefore, it is expected that at least the first protonation steps take place on the polyamine chain. This hypothesis is confirmed by the analysis of the absorption spectra recorded on solutions containing **L2** and **L3** at various pH values (Figure 2a,b). The absorption spectra are similar to the dipyridine chromophore. As observed for 2,2′-bipyridine alone, protonation of the heteroaromatic nitrogens gives rise to a new red-shifted absorption band in both **L2** and **L3**, with $\lambda_{max} = 313$ and 304 nm, respectively. According to Figure 2a, for **L2** this occurs upon protonation of the fifth nitrogen. On the other hand, in the case of **L3** a small change in the shape of the absorption spectra is visible after the third protonation step. This suggests that at least a partial localization of positive charge occurs on the heteroaromatic nitrogen in the $[H_3\mathbf{L3}]^{3+}$ species. The inset of Figure 2b shows a clear increase of the absorption at 304 nm as the pH decreases, i.e., with the formation of species with increasing protonation degree. To get further insight into the stepwise protonation of both ligands, we recorded ^{1}H and ^{13}C NMR spectra on aqueous solutions containing **L2** or **L3** at different pH values. In the case of **L2**, protonation of the ligand does not markedly affect either the chemical shift or the shape of the signals of aromatic nitrogens from alkaline pH values up to pH 3, where the formation of the pentaprotonated species $[H_5\mathbf{L2}]^{5+}$ takes place in solution (see the inset of Figure 2a). On the other hand, in the same pH range, significant downfield shifts are observed for the protons of the aliphatic chains. These data indicate that the first four protonation steps take place on the amine groups of the aliphatic chain, where the heteroaromatic nitrogens are not involved in protonation. Below pH 3 a remarkable downfield shift (ca 0.3 ppm) is instead observed for the aromatic protons, suggesting that the fifth protonation step directly involves the dipyridine unit.

A rather different protonation behavior is found in the case of **L3**. Figure 3 reports the ^{1}H chemical shifts of **L3** at different pH values (see Scheme 2 for labeling). The number of the ^{1}H and ^{13}C signals is in accord with a C_{2v} time-averaged symmetry in aqueous solutions throughout all the pH range investigated. In the pH range 12−8, where two protons bind to the ligand, the signals of the hydrogen H10, H11, and H9, in the α-position with respect to N3 and N4, exhibit a marked downfield shift; minor shifts are observed for the other signals. The formation of the $[H_2\mathbf{L3}]^{2+}$ species is also accomplished by a sensible upfield shift of the resonances of the carbon atoms C10, and C11 and C8, in the β-position with respect to N3 and N4, respectively, in good agreement with the β-shift reported for protonation of polyamines.[32] This strongly suggests that in $[H_2\mathbf{L3}]^{2+}$ the acidic protons are shared between the amine groups N4, N3, and N3′, as drawn in Scheme 2.

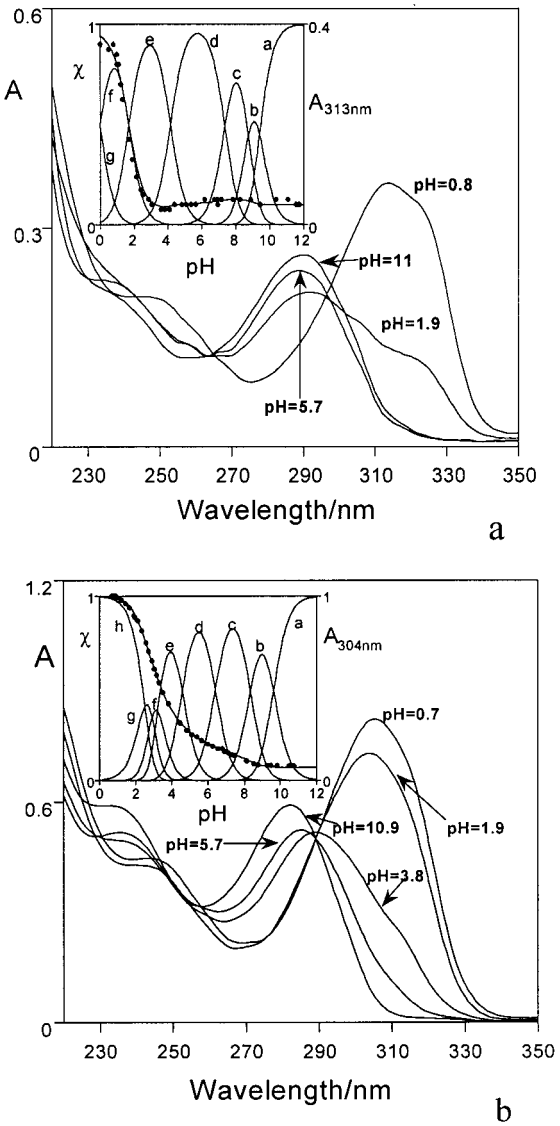

Figure 2. (a) pH dependence of the absorption spectra of **L2** ([**L2**] = 2.1×10^{-5} M, $I = 0.1$ M) Inset: absorbance at 313 nm (●) and molar fractions (χ) of the protonated forms of **L2** (dashed lines) (a = **L2**, b = H**L2**$^{2+}$, c = $H_2\mathbf{L2}^{2+}$, d = $H_3\mathbf{L2}^{3+}$, e = $H_4\mathbf{L2}^{4+}$, f = $H_5\mathbf{L2}^{5+}$, g = $H_6\mathbf{L2}^{6+}$). (b) pH dependence of the absorption spectra of **L3** ([**L3**] = 5.4×10^{-5} M, $I = 0.1$ M) Inset: absorbance at 304 nm (●) and molar fractions (χ) of the protonated forms of **L3** (dashed lines) (a = **L3**, b = H**L3**$^{+}$, c = $H_2\mathbf{L3}^{2+}$, d = $H_3\mathbf{L3}^{3+}$, e = $H_4\mathbf{L3}^{4+}$, f = $H_5\mathbf{L3}^{5+}$, g = $H_6\mathbf{L3}^{6+}$, h = $H_7\mathbf{L3}^{7+}$).

In the pH range 7.5−4, where the triprotonated and tetraprotonated species $[H_3\mathbf{L3}]^{3+}$ and $[H_4\mathbf{L3}]^{4+}$ are formed, large downfield shifts affect the resonance of the benzylic protons H7 and H8, adjacent to N2, and those of the aromatic protons H3, H5, and H2, while the signals of H9, H10, and H11, adjacent to N3 and N4, does not appreciably shift. In the same pH range, the ^{13}C spectra show a remarkable upfield shift for the C4 signal, in the β-position to N2. These spectral features indicate that the third and fourth protonation steps mainly involve the benzylic nitrogens N2 and N2′ and the heteroaromatic nitrogens of the dipyridine unit, as already proposed on the basis of the

(32) Batchelor, J. C.; Prestegard, J. H.; Cushley, R. J.; Lipsy, S. R. *J. Am. Chem. Soc.* **1973**, *95*, 6558. (b) Quirt, A. R.; Lyerla, J. R.; Peat, I. R.; Cohen, J. S.; Reynold, W. R.; Freedman, M. F. *J. Am. Chem. Soc.* **1974**, *96*, 570. (c) Batchelor, J. C. *J. Am. Chem. Soc.* **1975**, *97*, 3410. (d) Sarnessky, J. E.; Surprenant, H. L.; Molen, F. K.; Reilley, C. N. *Anal. Chem.* **1975**, *47*, 2116.

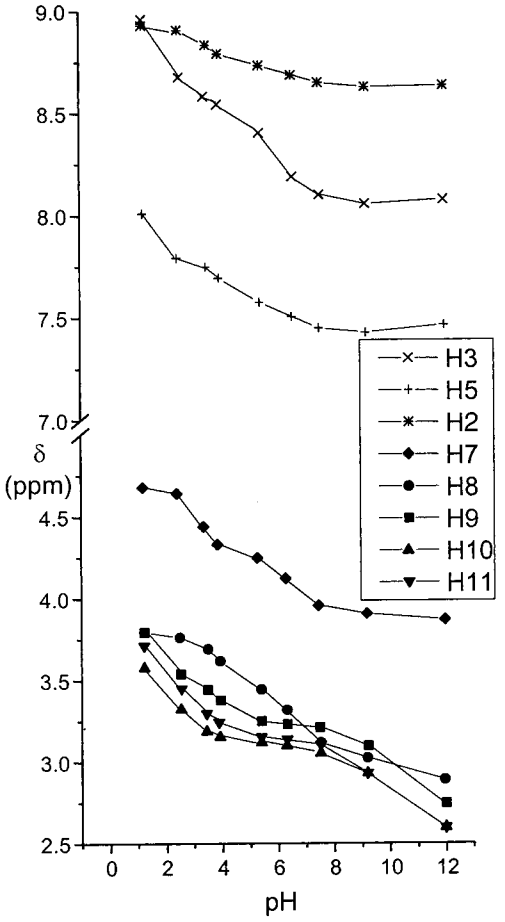

Figure 3. ^{1}H chemical shifts of the **L3** signals as a function of pH.

Scheme 2

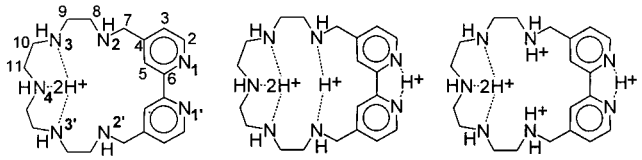

UV spectral data. In $[H_4\mathbf{L3}]^{4+}$, therefore, one acidic proton is localized on the heteroaromatic nitrogens and the other three on the pentaamine chain, as actually shown by the crystal structure of $[H_4\mathbf{L3}](ClO_4)_4$. The marked downfield shift of the signal of H7 below pH 3.5 indicates that the fifth protonation step mainly involves, once again, the benzylic nitrogens N2 and N2′ (Scheme 2). Although the NMR spectra do not allow discernment of the sixth and the seventh protonation sites, it is obvious that the last two protonation steps take place on the remaining amine group of the N3−N4−N3′ chain and on the dipyridine nitrogens. A crystal structure of the $[H_6\mathbf{L3}](NO_3)_6$ salt[33] shows that one of the dipyridine nitrogen is not protonated, suggesting that the sixth protonation step occurs on the N3−N4−N3′ moiety.

The most interesting finding is the fact that protonation of **L3** takes place on the heteroaromatic moiety from the third protonation step. Protonation of dipyridine implies localization of the acidic proton outside the cavity and allows a better minimization of the repulsion between positive charges.

(33) Bazzicalupi, C. Unpublished results.

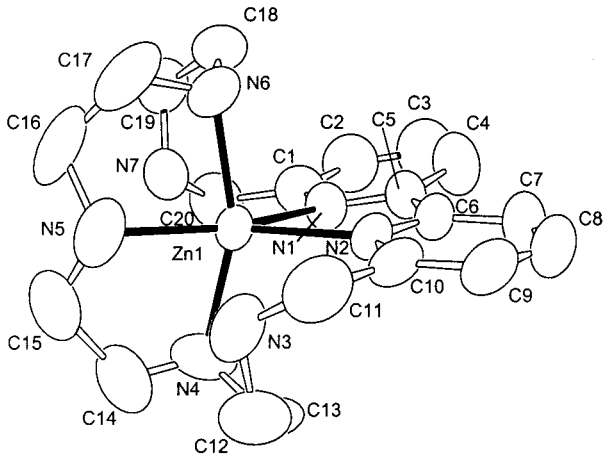

Figure 4. ORTEP drawing of the $[Zn\mathbf{L2}]^{2+}$ cation.

Table 2. Selected Bond Lengths (Å) and Angles (deg) for $[ZnL2](ClO_4)_2$

Zn(1)−N(4)	2.125(4)	N(6)−Zn(1)−N(5)	80.18(19)
Zn(1)−N(6)	2.141(4)	N(4)−Zn(1)−N(1)	99.82(14)
Zn(1)−N(5)	2.176(4)	N(6)−Zn(1)−N(1)	94.50(16)
Zn(1)−N(1)	2.239(3)	N(5)−Zn(1)−N(1)	154.71(15)
Zn(1)−N(2)	2.275(3)	N(4)−Zn(1)−N(2)	102.64(16)
N(4)−Zn(1)−N(6)	159.03(18)	N(6)−Zn(1)−N(2)	96.20(13)
N(4)−Zn(1)−N(5)	80.34(19)	N(5)−Zn(1)−N(2)	132.32(15)
		N(1)−Zn(1)−N(2)	72.63(12)

Zn(II) Complexation by L2 and L3. Crystal Structure of $[ZnL2](ClO_4)_2$. The molecular structure of $[Zn\mathbf{L2}](ClO_4)_2$ consists of $[Zn\mathbf{L2}]^{2+}$ complex cations and perchlorate anions. Figure 4 shows an ORTEP[31] drawing of the cation with atom labeling and Table 2 lists bond lengths and angles for metal coordination. The zinc atom is pentacoordinated by the heteroaromatic nitrogens N1 and N2, and by the N4, N5, and N6 nitrogen donors of the aliphatic chain. The coordination geometry can be best described as a distorted trigonal bipyramid. The two dipyridine nitrogens and the central amine group of the aliphatic chain, N5, define the equatorial plane of the bipyramid, while N4 and N6 occupy the apical positions. The two benzylic nitrogen N3 and N7 lie at longer distance (Zn1···N7, 2.517(3) Å; Zn1···N3, 2.768(4) Å) and are not involved in metal coordination. The amine group N3 is involved in a intramolecular hydrogen bond with N5 (N3···N5, 2.904(7) Å). Considering the ligand conformation, the macrocycle presents a noncrystallographic C_2 symmetry, with the C_2 axis approximately passing through the N5 and Zn1 atoms and bisecting the C5−C6 bond. The two aromatic rings are not coplanar, forming a dihedral angle of 9.9(1)°. The aliphatic polyamine chains C20−N7−C19−C18−N6 and C11−N3−C12−C13−N4 point in opposite directions with respect to the mean plane defined by the dipyridine unit. The amine groups N3, N4, N6, and N7 are almost coplanar (max. deviation 0.107(4) Å for N4). This plane is almost perpendicular to the mean plane defined by the heteroaromatic units, forming a dihedral angle of 77.8(1)°. Such a disposition gives rise to an overall screw conformation of the macrocycle, which allows the ligand to wrap around the metal cation.

Zn(II) Coordination in Aqueous Solution. Zn(II) coordination by **L2** and **L3** was studied by means of potentiometric measurements, and the stability constants of the complexes formed in aqueous solutions are listed in Table 3. Both ligands can form mono- and dinuclear Zn(II) complexes in aqueous solution.

Table 3. Stability Constants of the Zn(II) Complexes (log K) with L2 and L3 (0.1 M NMe_4Cl, 298.1 K)

reaction	log *K* L2	L3
$\mathbf{L} + Zn^{2+} = [Zn\mathbf{L}]^{2+}$	12.11(4)	8.95(6)
$[ZnL]^{2+} + H^+ = [Zn\mathbf{L}H]^{3+}$	7.10(1)	8.31(6)
$[ZnLH]^{3+} + H^+ = [Zn\mathbf{L}H_2]^{4+}$	5.22(3)	7.18(5)
$[ZnLH_2]^{4+} + H^+ = [Zn\mathbf{L}H_3]^{5+}$		5.43(4)
$[ZnLH_3]^{5+} + H^+ = [Zn\mathbf{L}H_4]^{6+}$		4.00(6)
$[ZnL]^{2+} + OH^- = [Zn\mathbf{L}(OH)]^{+}$	3.05(5)	4.16(3)
$[ZnL(OH)]^{+} + OH^- = [Zn\mathbf{L}(OH)_2]$		2.85(8)
$[ZnL]^{2+} + Zn^{2+} = [Zn_2\mathbf{L}]^{4+}$	4.61(7)	5.33(6)
$[Zn_2L]^{4+} + OH^- = [Zn\mathbf{L}(OH)]^{3+}$	5.88(8)	
$[Zn_2L(OH)]^{3+} + OH^- = [Zn_2\mathbf{L}(OH)_2]^{2+}$	5.19(7)	

Mononuclear Zn(II) Complexes. Considering the data in Table 3, it is to be noted that the stability constants of the $[Zn\mathbf{L}]^{2+}$ complexes ($\mathbf{L} = \mathbf{L2}$ and **L3**) are rather low considering the large number of nitrogen atoms which could be involved in metal coordination. It can be of interest to compare the stability constant of the present mononuclear complexes with that of the Zn(II) complexes with the macrocyclic ligand 1,4,7,10,13,16,-19-heptaazacycloheneicosane (**L4**),[34] which contains seven secondary amine groups linked by ethylenic chains, and 2,5,8,-11,14-pentaaaza[15]-16,29-phenanthrolinophane (**L1**),[29b] where a 2,9-phenanthroline unit replaces the bipyridine moiety. The formation constant of the **L2** complex is somewhat lower than that of **L4** (log $K = 12.11$ for $[Zn\mathbf{L2}]^{2+}$, Table 3, vs log $K = 13.33$ for $[Zn\mathbf{L4}]^{2+}$) and almost equal to that of **L1** (log $K = 12.38$ for $[Zn\mathbf{L1}]^{2+}$). The rather low stability of the **L1** and **L4** complexes was explained by considering the formation of large chelate rings due to the presence of some nitrogen donors not bound to the metal. A similar assumption can be also made in the case of the present $[Zn\mathbf{L2}]^{2+}$ complex. This is supported by the high values of the equilibrium constants for successive addition of H^+ to the $[Zn\mathbf{L2}]^{2+}$ complex, which suggest that protonation takes place on uncoordinated nitrogen atoms. Furthermore, the crystal structure of the $[Zn\mathbf{L2}]^{2+}$ cation shows the metal cation coordinated by the dipyridine nitrogens and three aliphatic amine groups, while the two benzylic amine groups are not bound. Most likely, as previously found in phenanthroline-containing macrocycles,[29] the rigidity of the dipyridine unit does not allow the simultaneous involvement in metal binding of the heteroaromatic nitrogens and the adjacent benzylic amine groups.

The most significant differences in Zn(II) coordination between ligands **L2** and **L3** are the marked lower stability of the $[Zn\mathbf{L3}]^{2+}$ complex and its tendency to form highly protonated species in aqueous solution (Table 3). In particular, the first three protonation constants of the complex are remarkably higher than that reported for 2,2′-dipyridine alone (log $K = 4.39$),[35] suggesting that at least in the $[Zn\mathbf{L3}H_3]^{5+}$ complex the three acidic protons are located on the polyamine chain. These data may indicate that in the highly protonated Zn(II) complexes the metal ion is located outside the cavity, coordinated by the heteroaromatic nitrogen donors of dipyridine. On the other hand, the stability constant of the $[Zn\mathbf{L3}]^{2+}$ is by far higher than those reported for the Zn(II) complex with 2,2′-dipyridine (log $K = 8.95$ for $[Zn\mathbf{L3}]^{2+}$ vs log $K = 5.0$ for $[Zn(2,2'\text{-dipyridine})]^{2+}$),[36] suggesting a different coordination mode of the metal in the unprotonated complex with respect to its protonated species.

To shed further light on the coordination features of these ligands, we carried out a UV−vis spectrophotometric and luminescence emission study on solutions containing Zn(II) and **L2** and **L3** in equimolecular ratio.

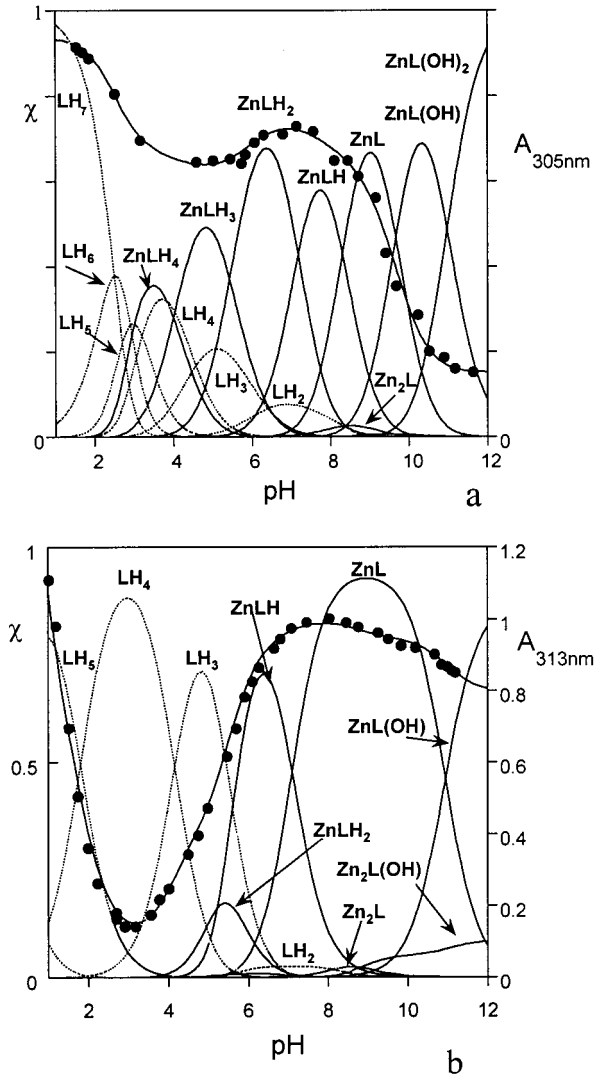

Figure 5. (a) Absorbance at 313 nm (●) and molar fractions (χ) of the protonated and complexed of **L2** (dashed lines) in the presence of Zn(II) (1:1 molar ratio) as a function of pH ($[\mathbf{L2}] = [Zn(II)] = 2.1 \times 10^{-5}$ M, $I = 0.1$ M). (b) absorbance at 305 nm (●) and molar fractions (χ) of the protonated and complexed species of **L3** (dashed lines) in the presence of Zn(II) (1:1 molar ratio) as a function of pH ($[\mathbf{L3}] = [Zn(II)] = 2.5 \times 10^{-5}$ M, $I = 0.1$ M).

As previously observed in the case of proton binding by 2,2-dipyridine, Zn(II) coordination by this heteroaromatic unit leads to dramatic changes in the absorption spectra of ligands **L2** and **L3**, with the appearance of new red-shifted absorption bands at ca. 313 nm for **L2** and 305 nm for **L3** (Figure S1, Supporting Information). These new bands can be used as a diagnostic tool to prove the effective involvement of dipyridine in metal binding. Parts a and b of Figure 5 display the variation of the molar absorbance at 313 and 305 nm for the **L2** and **L3** complexes, respectively, as a function of pH. Figure 5a clearly shows a marked decrease of the adsorbance with the formation of the $[H_4\mathbf{L2}]^{4+}$ species at pH ca. 2, as observed in the spectrophotometric titration of the ligand in the absence of Zn-(II), followed by an absorption increase at slightly acidic pH values, where the formation of the Zn(II) complex, in its mono and diprotonated forms, takes place in solution. Therefore, in the $[Zn\mathbf{L2}]^{2+}$ complex as well as in its protonated species, the metal is enclosed within the ligand cavity, coordinated by the

(34) Bencini, A.; Bianchi, A.; Dapporto, P.; Garcia-España, E.; Micheloni, M.; Paoletti, P. *Inorg. Chem.* **1989**, *28*, 1188.
(35) Odani, A.; Masuda, H. *J. Am. Chem. Soc.* **1992**, *114*, 6294
(36) Mohan, M.; Bancroft, D.; Abbott, E. *Inorg. Chem.* **1979**, *18*, 2468.

Scheme 3

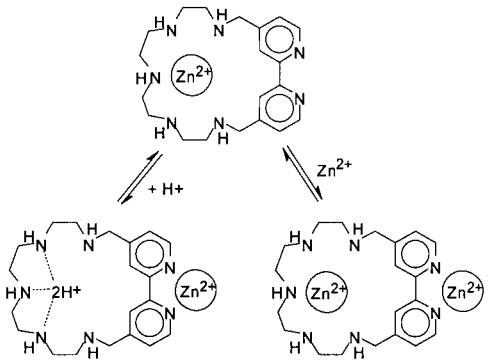

heteroaromatic moiety, in good accord with the results derived from the potentiometric study of this system as well as with the crystal structure of the $[Zn\mathbf{L2}]^{2+}$ cation.

A decrease of the absorbance in the pH range 1−4 is also observed in the case of **L3** (Figure 5b). In this pH range highly protonated species of the ligand are prevalent in aqueous solution, and the decrease in absorbance is mainly due to partial deprotonation of the dipyridine unit passing from $[H_5\mathbf{L3}]^{5+}$ to $[H_3\mathbf{L3}]^{3+}$. Such a decrease, however, is much less marked than in the case of **L2**, due to simultaneous formation of the tetra- and triprotonated forms of the complex, $[Zn\mathbf{L3}H_4]^{6+}$ and $[Zn\mathbf{L3}H_3]^{5+}$. Above pH 4 the formation of the diprotonated species of the complex, $[Zn\mathbf{L3}H_2]^{4+}$, gives rise, once again, to an increase of the absorbance. These data account for the involvement of the dipyridine unit in metal coordination in the protonated forms of this Zn(II) complex. In other words, in the protonated complexes, the metal is lodged outside the cavity, coordinated by the heteroaromatic nitrogens, while the acidic protons are bound by the polyamine chain (Scheme 3).

The most interesting finding, however, is the sharp decrease of the absorbance at alkaline pHs, occurring upon the formation of the $[Zn\mathbf{L3}]^{2+}$ complex and its mono- and dihydroxo complexes. Such a behavior implies that in the nonprotonated forms of the complex the dipyridine unit is not involved in metal coordination and Zn(II) is lodged inside the macrocyclic cavity. The particular molecular topology of this ligand gives rise to a pH-controlled change of binding site for the metal, which translocates from inside to outside the cavity upon protonation of the $[Zn\mathbf{L3}]^{2+}$ complex.

The process of complex formation was also followed by means of fluorescence emission spectra at different pH values. Different from the Zn(II) complex of 2,2′-dipyridine, which is known to exhibit a strong fluorescence emission, no luminescence was observed for the Zn(II) complex with **L2**. This behavior can be ascribed, once again, to the fact that the benzylic amine groups are not involved in metal coordination, leaving their lone pair available for the quenching of the emission via a photoinduced electron transfer process. An identical effect was recently reported for the Zn(II) complexes with phenanthroline-containing macrocycles, such as **L1**.[29]

The Zn(II) complex with **L3** shows a different behavior. Figure 6a displays the fluorescence emission spectra at different pH values. The most interesting finding is the appearance of a strong emission at 316 nm at slight acidic pH, with a maximum at pH ca. 5. As shown in Figure 6b, this emission can be attributed to the formation of the tetraprotonated and triprotonated $[Zn\mathbf{L3}H_4]^{6+}$ and $[Zn\mathbf{L3}H_3]^{5+}$ species, while the less protonated species are only weakly emissive. This result points out that in the $[Zn\mathbf{L3}H_2]^{4+}$ and $[Zn\mathbf{L3}H]^{3+}$ complexes at least one of the benzylic amine groups is not protonated and, therefore, available to carry out the quenching of the excited state by electron transfer. A total quenching of emission is observed at alkaline pH values, due to the formation of the $[Zn\mathbf{L3}]^{2+}$ complex and its hydroxylated species, where the metal is lodged inside the macrocyclic cavity (Figure 6b). Therefore, "jumping" of the metal between the two coordinative sites of the chemosensor **L3** determines an on/off switching of its fluorescence emission.

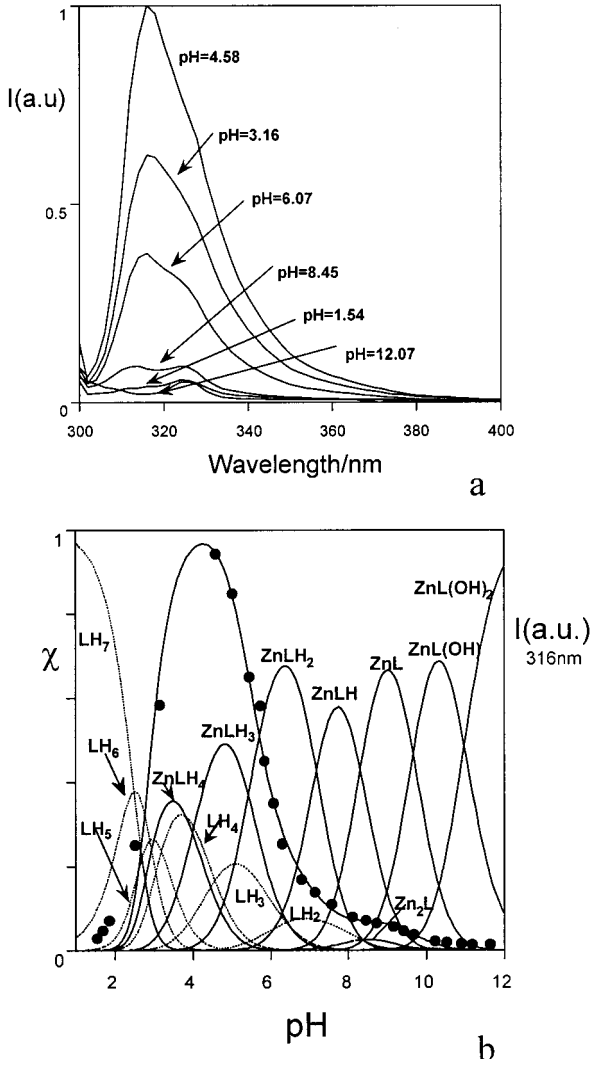

Figure 6. (a) Fluorescence emission spectra of the Zn(II) complexes with **L3** at different pH values (excitation wavelength of 293 nm). (b) fluorescence emission (●) and molar fractions (χ) of the protonated and complexed species of **L3** (dashed lines) in the presence of Zn(II) (1:1 molar ratio) as a function of pH ($[\mathbf{L}] = 2.5 \times 10^{-5}$ M; $I = 0.1$ M).

Dinuclear Zn(II) Complexes. As previously observed, both ligands can form dinuclear metal complexes in aqueous solution. In the case of **L2**, the constant for the addition of the second metal to the $[Zn_2\mathbf{L2}]^{4+}$ complex is by far lower than the formation constant of the $[Zn\mathbf{L2}]^{2+}$ (4.61 vs 12.11 log units, Table 3), as expected considering that two metal cations are lodged at short distance inside the macrocyclic cavity. It is worth noting that the $[Zn_2\mathbf{L2}]^{4+}$ complex shows a marked tendency to form mono- and dihydroxo species in aqueous solution. The constants for successive addition of OH^- anions to the $[Zn_2\mathbf{L2}]^{4+}$ complex are high (5.88 and 5.19 log units) in comparison with the analogous constants for the addition of hydroxo groups to the corresponding mononuclear $[Zn\mathbf{L2}]^{2+}$ complex ($\log K = 3.05$, see Table 3). This indication of a strong

binding of the hydroxide ion leads us to suppose that this group bridges the two metal centers. Different from the mononuclear Zn(II) complex, the dinuclear **L2** complex displays a fluorescence emission. A simple titration carried out by successive addition of Zn(II) to an aqueous solution of the ligand at pH 7.5 shows the appearance of an emission band at ca. 320 nm for metal to ligand molar ratios greater than 1, i.e., with the formation of the $[Zn_2\mathbf{L2}]^{4+}$ complex. This feature may indicate that in the dinuclear complexes all nitrogen donors are involved in metal coordination and, therefore, are not available for the process of emission quenching.

The dinuclear Zn(II) complex with **L3** displays, once again, a different behavior. First, the difference between the stability constants of the $[Zn\mathbf{L3}]^{2+}$ and the $[Zn_2\mathbf{L3}]^{4+}$ complexes (8.95 vs 5.33 log unit) is remarkably lower with respect to the Zn(II) complexes with **L2**. Furthermore, the constant for the addition of the second Zn(II) to the $[Zn\mathbf{L3}]^{2+}$ is very similar to that reported for Zn(II) complexation with 2,2′-dipyridine (4.95 log units). These data indicate that the second Zn(II) ion coordinates to the dipyridine unit, giving rise to a dinuclear complex in which the two metals occupy the two separated binding zones of **L3** (Scheme 3). Interestingly, this dinuclear complex is not emissive, suggesting that in the $[Zn_2\mathbf{L3}]^{4+}$ complex at least one aliphatic amine group is not coordinated to the metal.

Concluding Remarks. The different molecular architecture of the two dipyridine-containing macrocycles **L2** and **L3** strongly affects their coordination features toward Zn(II) as well as the photophysical properties of the complexes. The formation of $[Zn\mathbf{L2}]^{2+}$ is accomplished by the appearance of a typical red-shifted absorption band at 313 nm, due to Zn(II) coordination to the dipyridine unit, inside the macrocyclic cavity. At the same time, this complex does not display fluorescence emission. As shown by the crystal structure of the $[Zn\mathbf{L2}]^{2+}$ cation, the benzylic amine groups do not bind to the metal and are available for the quenching emission through an electron-transfer process. In the case of **L3**, in the protonated $[Zn\mathbf{L3}H_x]^{2+x}$ complexes, formed at acidic pHs, the metal is coordinated to the dipyridine nitrogens outside the cavity. In fact, these complexes display a new red-shifted band at 305 nm in the absorption spectra and give fluorescence emission, at least in the highest protonation degrees. In $[Zn\mathbf{L3}]^{2+}$, $[Zn\mathbf{L3}(OH)]^{+}$, and $[Zn\mathbf{L3}(OH)_2]$, formed at alkaline pH values, the dipyridine is not involved in metal coordination and the Zn(II) ion is coordinated to the amine groups inside the macrocyclic cavity, as shown by the decrease of the absorption at 305 nm and by quenching of the fluorescence emission observed in the alkaline pH region. Therefore, the particular molecular topology of this ligand gives rise to a pH-controlled translocation of the metal from outside to inside the cavity.

The dinuclear Zn(II) complexes with **L2** and **L3** also show different structural features. While in $[Zn_2\mathbf{L2}]^{4+}$ both metals are lodged inside the macrocyclic cavity, in $[Zn_2\mathbf{L3}]^{4+}$ one of the metal ions is coordinated by the heteroaromatic nitrogens outside the macrocyclic cavity.

Experimental Section

Synthesis. Ligand **L2**,[37] 4,4′-bis(bromomethyl)-2,2′-bipyridine[38] (**1**), and 1,4,7,10,13-pentakis(*p*-tolylsulfonyl)-1,4,7,10,13-pentaazatridecane[39] (**2**) were synthesized as previously described.

Table 4. Crystal Data and Structure Refinement for $[H_4\mathbf{L3}](ClO_4)_4{\cdot}H_2O$ (a) and $[Zn\mathbf{L2}](ClO_4)_2$ (b)

	a	b
empirical formula	$C_{20}H_{37}Cl_4N_7O_{17}$	$C_{20}H_{31}Cl_2N_7O_8Zn$
formula weight	789.37	633.79
temperature, K	298	298
wavelength, Å	0.71069	1.54180
space group	$P\bar{1}$	$P2_1/c$
a, Å	8.758(9)	11.848(1)
b, Å	9.662(3)	11.276(1)
c, Å	19.190(7)	19.688(3)
α , deg	91.17(3)	90
β, deg	97.12(5)	94.01(1)
γ, deg	94.23(5)	90
volume, Å^3	1606.2(18)	2623.8(5)
Z	2	4
calcd density, Mg/m^3	1.632	1.604
absorption coeff, mm^{-1}	0.455	3.694
crystal size, mm	0.35 × 0.3 × 0.1	0.4 × 0.4 × 0.3
final R indices [$I > 2\sigma(I)$][a]	R1 = 0.0672 wR2 = 0.1795	R1 = 0.0574 wR2 = 0.1707
R indices (all data)[a]	R1 = 0.1056 wR2 = 0.1957	R1 = 0.0635 wR2 = 0.1772

[a] $R1 = \sum||F_o| - |F_c||/\sum|F_o|$; $wR2 = [\sum w(F_o^2 - F_c^2)^2/\sum wF_o^4]^{1/2}$.

4,4′-(2,5,8,11,14-Pentatosyl-2,5,8,11,14-pentaaza[15])-2,2′-bipyridylophane (3). A solution of **1** (6 g, 17.5 mmol) in dry CH_3CN (500 cm^3) was added over a period of 4 h to a refluxing and vigorously stirred suspension of **2** (16.8 g, 17.5 mmol) and K_2CO_3 (28 g, 0.20 mol) in CH_3CN (1 L). After the addition was completed, the solution was refluxed for additional 2 h. The resulting suspension was filtered out and the solution was vacuum evaporated to give a crude solid. The product was recrystallized from toluene, affording **3** as a colorless solid. Yield: 14 g (70%). Anal. Found: C, 57.7; H, 5.4; N, 8.55. Anal. Calcd for $C_{55}H_{61}N_7S_5O_{10}$: C, 57.93; H, 5.39; N, 8.6. ^{1}H NMR ($CDCl_3$) δ (ppm): 2.35 (s, 3H), 2.40 (s, 6H), 2.42 (s, 6H), 2.88 (m, 4H), 2.90 (m, 4H), 3.15 (m, 4H), 3.31 (m, 4H), 4.42 (s, 4H), 7.38 (m, 14H), 7.67 (d, 4H), 7.74 (d, 2H), 7.81 (d, 4H), 7.99 (d, 2H). ^{13}C NMR ($CDCl_3$) δ (ppm): 22.3, 47.9, 48.9, 49.4, 49.7, 55.4, 121.1, 124.7, 128.1, 128.6, 131.4, 135.4, 136.4, 137.5, 138.8, 145.2, 146.5, 156.0, 157.6.

4,4′-(2,5,8,11,14-Pentaaza[15])-2,2′-bipyridylophane Pentahydrobromide (L3 5HBr). Compound **3** (2.85 g, 2.46 mmol) and phenol (33 g, 0.350 mol) were dissolved in 33% HBr/CH_3COOH (250 cm^3). The reaction mixture was kept under stirring at 90 °C for 22 h until a precipitate was formed. The solid was filtered out and washed several times with CH_2Cl_2. The pentahydrobromide salt was recrystallized from a EtOH/water 2:1 mixture. Yield: 1.6 g (85%). Anal. Found: C, 30.9; H, 4.7; N, 12.5. Anal. Calcd for $C_{20}H_{36}N_7Br_5$: C, 31.03; H, 4.69; N, 12.67. ^{1}H NMR (D_2O, pH 4) δ (ppm): 2.24 (m, 4H), 2.37 (m, 4H), 3.36 (t, 4H), 3.61 (t, 4H), 4.76 (s, 4H), 7.88 (d, 2H), 8.06 (s, 2H) 8.59 (d, 2H). ^{13}C NMR (D_2O, pH 4) δ (ppm): 44.4, 44.6, 46.1, 53.3, 124.5, 128.3, 130.1, 140.2, 145.3, 152.3.

$[H_4\mathbf{L3}](ClO_4)_4{\cdot}H_2O$. To a solution of **L3** (18.5 mg, 0.05 mmol) in water (pH 4) was added $NaClO_4{\cdot}H_2O$ (100 mg, 0.7 mmol). Crystals of $[H_4\mathbf{L3}](ClO_4)_4{\cdot}H_2O$ suitable for X-ray analysis were obtained by slow evaporation of this solution. Yield: 25 mg (58%). Anal. Found: C, 30.3; H, 4.8; N, 12.3. Anal. Calcd for $C_{20}H_{37}Cl_4N_7O_{17}$: C, 30.43; H, 4.72; N, 12.42.

$[Zn\mathbf{L2}](ClO_4)_2$. $Zn(ClO_4)_2{\cdot}6H_2O$ (18.7 mg, 0.05 mmol) was added to a solution of **L2** (18.5 mg, 0.05 mmol) in methanol (10 cm^3), and then butanol (10 cm^3) was added. Crystals of $[Zn\mathbf{L2}](ClO_4)_2$ were obtained by slow evaporation of the solution. Yield: 30 mg (94%). Anal. Found: C, 38.2; H, 5.0; N, 15.5. Anal. Calcd for $C_{20}H_{31}Cl_2N_7O_8Zn$: C, 37.90; H, 4.93; N, 15.47.

X-ray Structure Analyses. Analyses on prismatic colorless single crystals of $[H_4\mathbf{L3}](ClO_4)_4{\cdot}H_2O$ (a) and $[Zn\mathbf{L2}](ClO_4)_2$ (b) were carried out with an Enraf-Nonius CAD4 and SIEMENS P4 X-ray diffractometers, respectively. Details for data collections and structure refinements are summarized in Table 4. Intensity data were empirically corrected for absorption (PSI−SCAN method). Both structures were

(37) Bencini, A.; Bianchi, A.; Fusi, V.; Giorgi, C.; Masotti, A.; Paoletti, P. *J. Org. Chem.* **2000**, *65*, 7686.
(38) Kaes, C.; Hosseini, M. W.;. De Cian A.; Fischer, J. *Tetrahedron Lett.* **1997**, 38, 4389.
(39) Bencini, A.; Bianchi, A.; Garcia-España, E.; Giusti, M.; Micheloni M.; Paoletti, P. *Inorg. Chem.* **1987**, *26*, 681.

solved by direct methods with the SIR97 program.[40] Refinements were performed by means of the full-matrix least-squares method with the SHELXL-97 program.[41]

X-ray Structure Determination of $[H_4L3](ClO_4)_4 \cdot H_2O$ (a). Anisotropic displacement parameters were used for all non-hydrogen atoms. All hydrogen atoms bound to carbon atoms were introduced in calculated positions with an overall isotropic thermal parameter refined to the final values of $U = 0.048(3)$ Å^2. The hydrogen atoms bound to the nitrogens were localized in the Fourier difference map, introduced in the calculation, and isotropically refined.

X-ray Structure Determination of $[ZnL2](ClO_4)_2$ (b). Anisotropic displacement parameters were used for all non-hydrogen atoms. Hydrogen atoms linked to N6 and to the carbon atoms were introduced in calculated position and their coordinates and isotropic thermal factors were refined in agreement with the linked atoms. Disorder was recognized for the C13−N4−C14−C15 chain, and double positions were used for all these atoms with population parameters 0.4 and 0.6. The hydrogen atoms bound to N4 and to the disordered carbon atom were not introduced in the calculation. Rotational disorder affects also a perchlorate ion. Two models, coincident in Cl3 and O33, were used to rationalize the disorder: the double positions for O31 and O34 (O31′ and O34′) were localized and introduced with the population parameter 0.5, while it was not possible to split the elongated ellipsoid of O32.

Potentiometric Measurements. Equilibrium constants for protonation and complexation reactions with **L2** and **L3** were determined by pH-metric measurements at 298.1 ± 0.1 K, by using equipment and procedures[26] which have been already described. $(1-2) \times 10^{-3}$ mol dm^{-3} ligands and metal ions concentrations were employed in the potentiometric measurements, varying the metal to ligand molar ratio from 0.5:1 to 2:1. Three titration experiments (about 100 data points for each one) were performed in the pH ranges 2.5−10.5. The computer program HYPERQUAD[42] was used to calculate equilibrium constants from emf data.

Spectrophotometric and Spectrofluorimetric Measurements. Absorption spectra were recorded on a Perkin-Elmer Lambda 6 spectrophotometer and fluorescence emission on a SPEX F111 Fluorolog spectrofluorimeter. HCl and NaOH were used to adjust the pH values, which were measured on a Metrohm 713 pH meter.

NMR and Electronic Spectroscopy. ^{1}H (300.07 MHz) and ^{13}C (75.46 MHz) spectra in D_2O solutions at different pH values were recorded at 298 K in a Varian Unity 300 MHz spectrometer. To adjust the pD, small amounts of 0.01 mol dm^{-3} NaOD or DCl solutions were added to solutions containing **L2** or **L3**. The pH was calculated from the measured pD values by using the following relationship pH = pD − 0.40.[43]

Acknowledgment. Financial support by the Italian Ministero dell′Università e della Ricerca Scientifica e Tecnologica, within the program COFIN 98, and by Italian Research Council (CNR) and PRAXIS contract 10074/98 (Portugal) are gratefully acknowledged.

Supporting Information Available: An X-ray crystallographic file, in CIF format is available. Tables listing detailed crystallographic data, atomic positional parameters, anisotropic temperature factors, and bond distances and angles for [Zn**L2**]$(ClO_4)_2$ and $[H_4$**L3**$](ClO_4)_4 \cdot H_2O$ are available. This material is available free of charge via the Internet at http/::pubs.acs.org.

IC001381K

(40) A. Altomare, A.; Burla, M. C.; Camalli, M.; Cascarano, G. L.; Giacovazzo, C.; Guagliardi, A.; Moliterni, A. G. G.; Polidori, G.; Spagna, R. *J. Appl. Crystallogr.* **1999**, *32*, 115.
(41) Sheldrick, G. M. SHELXL-97, University of Göttingen, Göttingen, 1997.
(42) Gans, P.; Sabatini, A.; Vacca, A. *Talanta* **1996**, *43*, 807−812.
(43) Covington, A. K.; Paabo, M.; Robinson, R. A.; Bates, R. G. *Anal. Chem.* **1968**, *40*, 700.